



euronoise

# Intensity fluctuations of mid-frequency sound signals passing through moving nonlinear internal wave in experiment sw06

Boris Katsnelson[a], Valery Grigorev[a], James Lynch[b] and Dajun Tang[c]

[a]Voronezh State University, 1, Universitetskaya sq., 394006 Voronezh, Russian Federation
[b]Woods Hole Oceanographic Institution, 98 Water Street, Bigelow 203A, MS-11, Woods Hole, MA 02543, USA
[c]Applied Physics Laboratory, University of Washington, 1013 NE 40th St, Seattle, WA 98105, USA
katz@phys.vsu.ru

**Abstract**. The fluctuations of intensity of broadband pulses in the mid-frequency range (2 – 4.5 kHz) propagating in shallow water in the presence of intense internal waves moving approximately along the acoustic track are considered. These pulses were received by two separate single hydrophone units (SHRUs) placed at different distances from the source (~4 km and ~12 km) and in different directions. It is shown that the frequency spectra of the fluctuations for these SHRUs have different predominating frequencies corresponding with the directions of the acoustic track. Comparison of experimental results with theoretical estimates demonstrate good consistency

# 1. Introduction. Statement of the problem

Fluctuations of the intensity of low frequency sound waves in the presence of intense internal waves moving along acoustic track were considered in papers [1] (experimental observations) and [2-4] (theoretical analysis). It was shown that the hypothesis of mode coupling as the physical reason for the fluctuations explains the peculiarities of the spectrum of these fluctuations (i.e., existence and value of a predominating frequency [2], the arrival times [3], etc.).

For mid and high frequency sound waves we should use ray language for the description of sound propagation in the presence of internal soliton (IS) moving along the acoustic track (paper [5]) as illustrated in Fig.1.

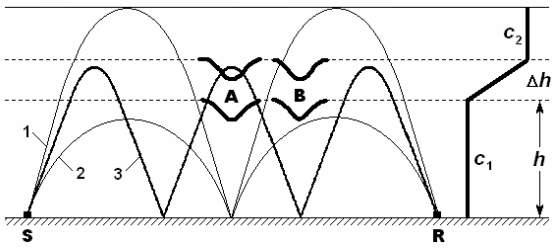


Fig 1. Schematic of the interaction of an internal soliton with sound rays of different types radiated from a source placed at the bottom. Sound speed profile on the right side corresponds to the simplified one for SW06. $h \sim 60$ m, $\Delta h \sim 10$ m, $c_1 \sim 1480$ m/s, $c_2 \sim 1525$ m/s

with trajectories of typical rays coming from the source to receiver as shown in Fig.1

Let us consider a source and receiver (S and R) of sound signals placed in shallow water with some distance between them

In the presence of internal solitons moving along the acoustic track, we have some moving perturbation of the thermocline layer and correspondingly some perturbation of the trajectory of the rays. This perturbation depends on the position of the IS and on the types of rays. For example, if the soliton is at position A, then it causes a distortion of ray 3, whereas for the position B of the soliton, ray 3 does not interact with it. So during the motion of the soliton we see temporal fluctuations of the sound intensity at the receiver. It is clear that the perturbation depends on the type of rays; for example, ray 3 interacts with the soliton more strongly than

rays 1 and 2. It has been shown that the most significant perturbation is provided by the rays which are tangent to the thermocline layer (we call these rays "critical rays," corresponding to ray 3 in Fig.1), whereas other rays (denoted as 1 and 2 in Fig.1) give a comparatively small contribution to the fluctuations. So if the velocity $v_t$ of the IS crest along the direction of the acoustic track (which is greater than the real velocity $v$ of the IS, which is perpendicular to the wave front of the IS) is taken to be constant, then the most significant fluctuations of the sound amplitude at the receiver will take place with a period $T_c$ determined by $v_t$ and the cycle distance of the critical ray $D_c$: $T_c = D_c / v_t$. For real ocean conditions, $T_c \geq 10$ min and so during the time of observation we can have 5-10 oscillations of the sound intensity. A spectrum of this signal taken during the time of observation (~ 60 min) should contain set of maxima spanned by the value $\Omega_c \sim v_t / D_c$. The value of $\Omega_c$ is the "frequency of collisions" of the IS with the critical ray and can also be called the "predominating frequency". For typical conditions, we have $\Omega_c \leq 10$ cph.

An important feature of this spectrum is the dependence of the predominating frequency $\Omega_c$ on the angle between the direction of the acoustic track and the direction of propagation of the IS. Using this, it is possible to check this theory with an experiment where we have two acoustic tracks with different directions (two receivers for one and the same source) if they are crossed by the same soliton (or train of solitons). In this case we should have fluctuations of the same sequence of signals with different predominating frequencies, corresponding to the projections of the real velocity or the direction of the acoustic track. As we will see below, such a situation took place in the SW06 experiment, along an acoustic track created by a source on the R/V KNORR.

# 2. Sallow water 06 experiment. Experimental data and analysis

The layout of the part of SW06 on 13 August during time period 15:31-16:20 GMT is shown in Fig.2.

Positions of the source (R/V KNORR), receivers (SHRU1 and SHRU2) and thermistor strings (SW23, SW24, SW30, SW31, SW54) are also shown in Fig.2.

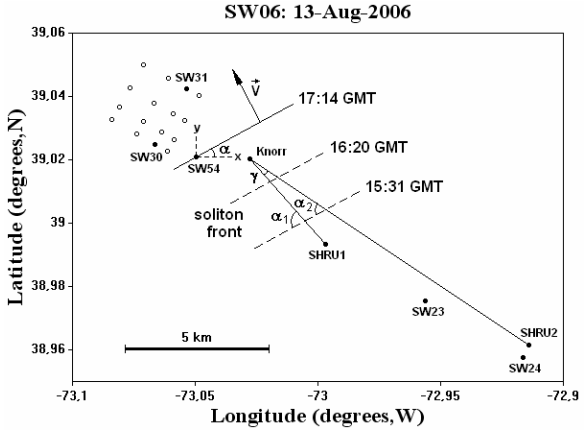


**Fig. 2**. Scheme of experiments with mid-frequency pulses in SW06. Black straight lines denote acoustic tracks 1 (Knorr-SHRU1) and 2 (Knorr-SHRU2)

The angle between the acoustic tracks is denoted by $\gamma$, and was found to be $\gamma \sim 15^o$.

The behavior of internal waves was monitored by several thermistor strings, moored at different places. For our purposes, we use the temporal records of temperature depth distribution from the sensors denoted SW23, 24,54,30,31 (see Fig.2 and 3). During this time period, some solitons were registered. In Fig.3 (a) we show three temperature records of the soliton, which is moving approximately toward the coast. We see that the moored sensors were reached by the first peak at different times (marked by arrows in Fig.3 (a)). The different shapes of the temperature distribution demonstrate the evolution of the soliton train in time and space. It is easily to estimate velocity and direction of propagation of the IS in a Cartesian coordinate system on the horizontal plane with the origin at mooring SW54. Suppose that the train or separate IS has a plane wave front directed at angle $\alpha$ with the X-axis, and moves with constant velocity $v$ (Fig.2,3). Given soliton consequently reaches sensor SW54, then SW30 and then SW31 ( Fig.4 (a)).

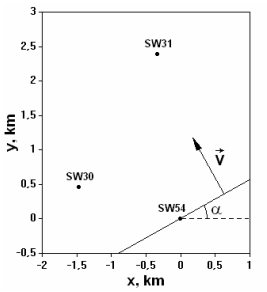


Fig.3

The corresponding time differences between the points SW30 and SW31 from one side and SW54 from other side are $\Delta T_{30} = 31$ min and $\Delta T_{31} = 63$ min. In this case:

$$\alpha = \arctan \frac{y_{30}\Delta T_{31} - y_{31}\Delta T_{30}}{x_{30}\Delta T_{31} - x_{31}\Delta T_{30}}$$

$$v = \frac{y_{30} - x_{30}\tan\alpha}{\Delta T_{30}} \cos\alpha$$

where $x_{30} = -1477$ m, $y_{30} = 456$ m, $x_{31} = -337$ m, $y_{31} = 2402$ m.

Taking into account experimental errors, we have approximately $\alpha \sim 29^\circ$, $v \sim 0.6$ m/s.

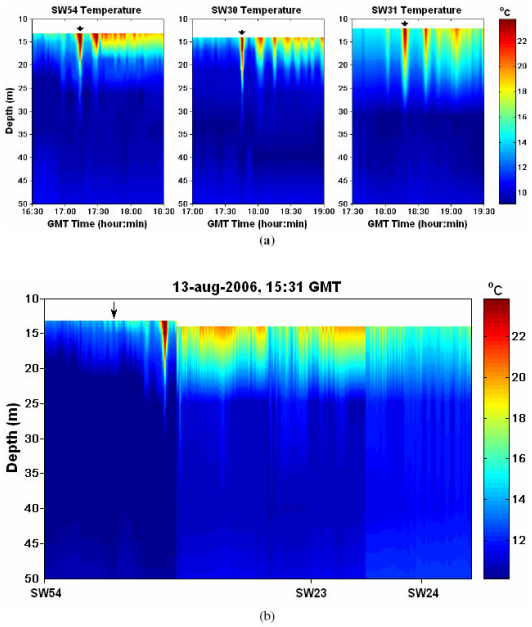


Fig.4. (a) Temperature records of an internal soliton at three thermistor strings. Color scale of temperature is shown at the right. (b) Reconstructed depth distribution of temperature for geotime 15:31 GMT along a straight line between thermistor's sensors SW24 – SW23 – SW54. Black arrow denotes position of the soliton at 16:20 GMT

Remark, that for more detail analysis of internal waves outside of acoustic track we can use 14 thermistors SW04 – SW17 (shown in Fig.2 by circles). In this case mentioned angle $\alpha$ changes during motion from right to left in area $26^\circ - 44^\circ$ as a result of variation of direction during propagation and bending of the wave front . At the same time along an acoustic track we have comparatively constant direction of wave front, and for the following work we take $\alpha \sim 29^\circ$.

Next we can reconstruct the spatial crossection of the internal waves along the straight line SW24-SW23-SW54 for some fixed time, for example 15:31 GMT. Let's denote temperature record at some point as $T^0(T, z)$, where $T^0$ is temperature and $T$ is geotime. Within the framework of our approximation, we have $T^0(T - T_0 - \frac{l - l_0}{v_l}, z)$, where $l$ is a length along the above mentioned direction, $v_l$ is the corresponding projection of the real velocity $v$, and $T_0$, $l_0$ are some fixed geotime and position of the internal waves. We note that in spite of Fig.3 (a) showing some evolution of the IS propagating toward the coast, during our time of processing (~1 hour) we can neglect this modification and consider the shape of the IS to be constant.

The reconstructed temperature distribution is shown in Fig.3 (b). We see that according to our environmental picture, there is only one separate soliton at both acoustic tracks: KNORR-SHRU1 and KNORR-SHRU2 for the time interval, (15:31-16:20 GMT). Positions of the wave front of the soliton for the geotimes 15:31 GMT and 16:20 GMT are shown in the Fig.2 by dotted lines and are also denoted in Fig.3(b) (soliton itself and black arrow). The velocity of the soliton along this direction is about 0.7 m/s.
During our geotime period, a sequence of pulses was radiated consisting of 200 separate pulses in the frequency band 2-10 kHz. See csheme or datiation in the Table 1)

Table.1 Intervals between pulses, which were numbered from 1 to 199

| Interval number | Duration of intervals ,s | Interval number | Duration of intervals, s |
|---|---|---|---|
| **1..42** | **14** | **100** | **150** |
| **43** | **15** | **101..102** | **14** |
| **44..46** | **14** | **103..104** | **15** |
| **47** | **15** | **105..122** | **14** |
| **48** | **14** | **123** | **15** |
| **49** | **15** | **124..148** | **14** |
| **50..76** | **14** | **149** | **15** |
| **77** | **16** | **150..154** | **14** |
| **78..85** | **14** | **155** | **16** |
| **86** | **15** | **156** | **15** |
| **87..98** | **14** | **157..181** | **14** |
| **99** | **15** | **182** | **15** |
| | | **183..199** | **14** |

Signiture of typical radiated pulse is shown in the Fig.5

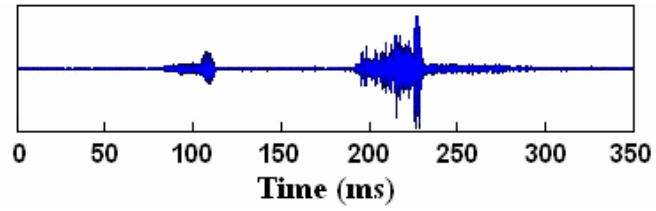


Fig.5

As was said above, these pulses were received independently at SHRU1 and SHRU2. The spectrum of radiated signals was in the band 2-10 kHz. However, for the processing, we use a sampling time $\delta t = 0.0001024$ sec, which corresponds to maximal frequency in the spectrum of $(2\delta t)^{-1} = 4.88$ kHz. So we will only consider the intensity of received pulses in the band 2-4 kHz. Our analysis above shows that the character of the fluctuations should not depend on the frequency in this band.
. Let the received pulse have the sound pressure signature $p(t)$ with the spectrum

$$S(\omega) = \int_0^{\tau} p(t)\exp(i\omega t)dt \qquad (1)$$

Here we take $\tau = 0.1$ sec (the approximate duration of the pulse) for both receivers.
Formally speaking we should take an infinite time period; but, it is more sensible to take this reduced period because outside of this interval we have noise only. So the energy of the pulse is

$$E = \int_{\omega_1}^{\omega_2} |S(\omega)|^2 d\omega \qquad (2)$$

where $\omega_1 = 2$ kHz, $\omega_2 = 4$ kHz.

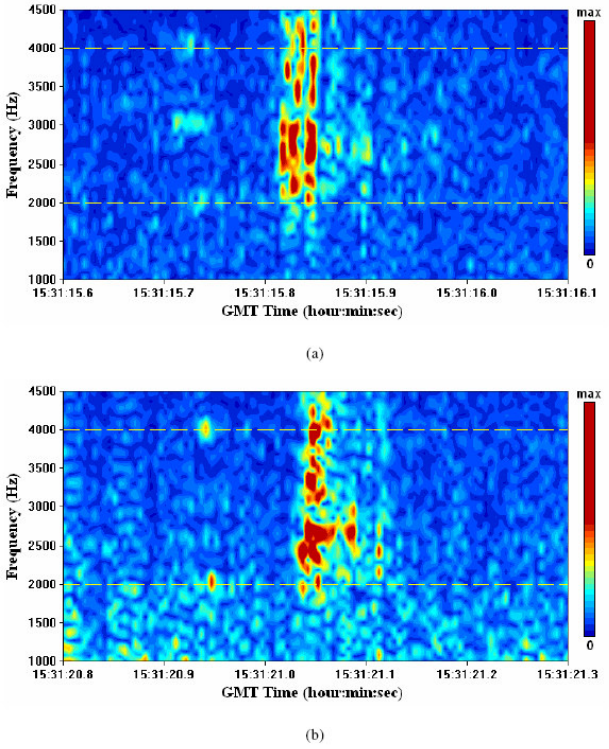


Fig.6 Spectrograms of one from 200 received pulses at the SHRU1 (a) and SHRU2 (b)

The energy of the received pulses fluctuates from pulse to pulse, as a function of geotime, so we denote it as $E = E(T)$. We can study the temporal dependence of the relative fluctuations using

$$\overline{E}(T) = \frac{E(T) - \langle E \rangle}{\langle E \rangle} \qquad (3)$$

where $\langle E \rangle = \frac{1}{\Delta T}\int_0^{\Delta T} E(T)dT$ is the average energy for the time period $\Delta T = 49$ min.
The temporal dependence of the fluctuations of energy for both hydrophones is shown in Fig.6

We see from Fig.7 (a,b) that the oscillations of the temporal dependence of the sound energy have a rather regular character. According to our theory [5], the frequency spectrum of the temporal behavior has

predominating frequencies, corresponding to the quasi-periodical
interaction of the sound pulse with the periodical ray structure of the sound field. The most significant interaction takes place for the critical ray, so the predominating frequency is determined by the time of motion of the pulse between adjacent maxima of the critical ray.

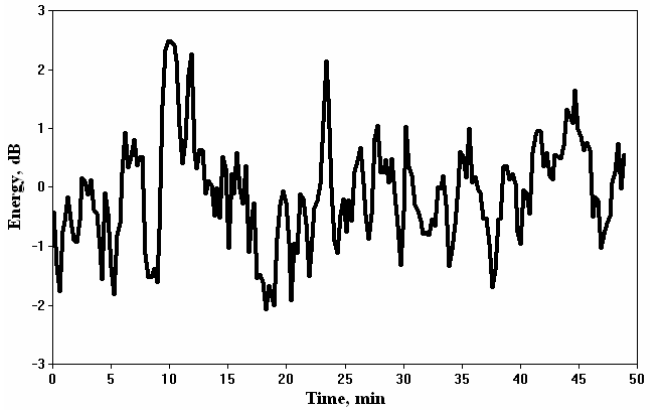


(a)

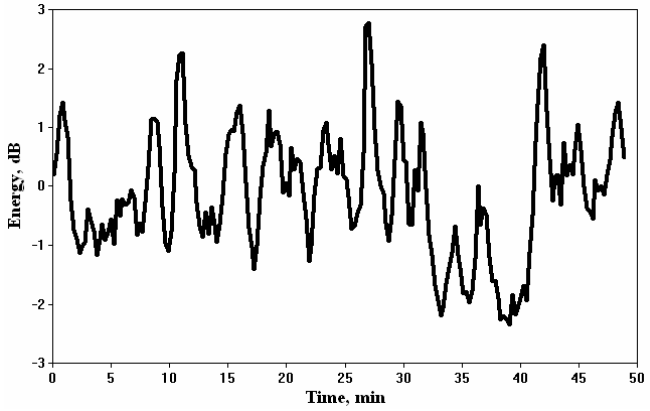


(b)

Fig. 7. Temporal dependence of the energy of the sound pulses for SHRU1 (a) and SHRU2 (b) for the time period 13 of August 2006, 15:31-16:20 GMT

Let's consider the spectrum of fluctuations, or more exactly the amplitude of this spectrum:

$$\overline{G}(\Omega)=\left|\int_0^{\Delta T}\overline{E}(T)\exp(i\Omega T)dT\right| \qquad (4)$$

The spectra for the temporal series from SHRU1 and SHRU 2 are shown in Fig.8 in dB units; more exactly, we show the values $10\log\overline{G}(\Omega)$.

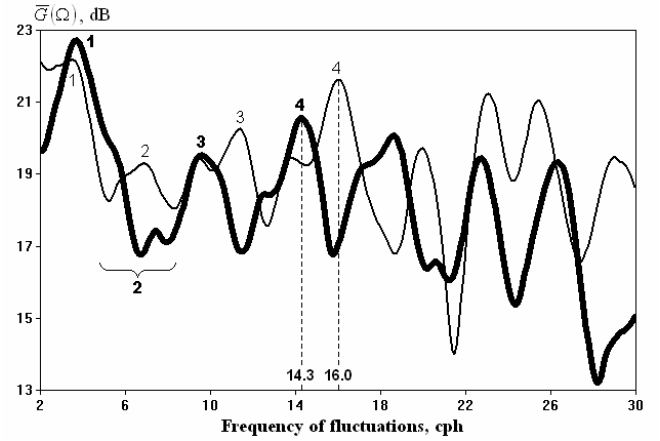


. Fig 8. Spectra of fluctuations of pulse energy. Bold line denotes spectrum for SHRU1, thin line corresponds to SHRU2. Dotted lines denote positions of the 4th harmonics of predominating frequencies

We can see that both spectra are functions having a quasi-periodical structure in the frequency domain in the region below 30 cph. We also see that the positions of the maxima in the spectra corresponding to SHRU1 and SHRU2 are shifted. According to our interpretation, this is due to the different directions of the sound propagation relative to the direction of propagation of the internal solitons.

The predominating frequencies and the average shifts of the spectra can be estimated from the experimental data (Fig.8). In particular maxima (harmonics) number 4 are shifted by 1.7 cph. For this case, $\Omega_c^1 \approx 3.58$ cph and $\Omega_c^2 \approx 4$ cph .

Let's consider the temporal dependence from the point of view of our theory, i.e. that motion of the soliton is the reason f

or the fluctuations with a predominating frequency, and compare the estimation from paper [5] with the results of our observations.

A diagram of the experiment showing all the relevant angles is found in Fig.2. We use the notation: $\gamma \sim 15^o$ is the angle between acoustic tracks 1 and 2; $\alpha_{1,2}$ are the angles between tracks 1 or 2 and the wave front of the IS correspondingly; these angles can be found if we know angle $\alpha$, so that we have $\alpha_1 \sim 78^o$, $\alpha_2 \sim 63^o$.

The velocities of the IS along acoustic tracks 1 and 2 can be calculated using the $v_{1,2} = v/\sin\alpha_{1,2}$. The corresponding predominating frequencies of fluctuation for the two acoustic tracks are then $\Omega_c^{1,2} = v/(D_c \sin\alpha_{1,2})$, In our case, for the sound speed profile in SW06 area, $D_c \sim 2hc_1/\sqrt{c_2^2-c_1^2} + 2\Delta h\sqrt{c_2^2-c_1^2}/\Delta c$. For our parameters, $D_c \sim 640$ m. Calculations give for frequencies $\Omega_c^1 \approx 3.45$ cph and $\Omega_c^2 \approx 3.8$ cph. These values are very close to the measured ones. We should remark that these values are sensitive to the value of the ray

cycle distance. However we can effectively exclude the ray cycle by considering only the ratio of the predominating frequencies:

$$\Omega_c^1 / \Omega_c^2 = \sin\alpha_2 / \sin\alpha_1 \qquad (5)$$

For our case, this ratio is $\sin\alpha_2 / \sin\alpha_1 \sim 0.91$ and for the experimental data it is $\Omega_c^1 / \Omega_c^2 = 0.895$, close to the aforementioned ratio.

# 3. Conclusion

The IS, moving approximately along an acoustic track, interacts with the quasi-periodical spatial interference pattern of the sound field formed by a set of rays (in the high frequency approximation) radiated from the source in a shallow water waveguide. Correspondingly, we have temporal fluctuations of the sound intensity at the receiver with frequency proportional to the velocity of the IS along the acoustic track. The difference in spectra of these fluctuations (shift of the predominating frequencies) for two acoustic tracks depends on the angle between them and we see good agreement with this hypothesis in the SW06 experiment.

It is very interesting, that the value of the predominating frequency does not depend (or depends weakly) upon the shape and amplitude of the IS, and on how many separate peaks there are in the train, and on its exact position between source and receiver. It is just this circumstance that allows us to get comparatively good agreement between theory and experiment.

In conclusion, we will note that this effect can also be used for solution of the inverse problem – to diagnose parameters of moving solitons (velocity and direction) on the basis of acoustical measurements with high (mid) frequency sources and two differently directed acoustic tracks.

# 4. Acknowledgements

The authors are very grateful to D.J.Tang for the information about radiated signals and helpful discussions. This work was supported by ONR, RFBR grant 06-05-64853 and CRDF (REC 010).

# References

[1] Badiey, M., Y. Mu, J. Lynch, J. R. Apel, and S.Wolf, "Temporal and azimuthal dependence of sound propagation in shallow water with internal waves," IEEE J. Oceanic Eng. 27(1), 117-129 (2002).

[2] Badiey M., Grigorev V., Katsnelson B., Lynch J "Perturbation of arrival times in sound pulses propagating in shallow water through moving internal solitons.", JASA, v.119 p.3225 (2006).

[3] Katsnelson B., Grigorev V., Badiey M., Lynch J. "Fluctuations of modal amplitudes due to modes coupling in shallow water", Journal of the Acoustical Society, v.120, p.3054 (2007).

[4] Katsnelson B., Grigorev V., Badiey M., Lynch J. "Temporal sound field fluctuations in presence of internal solitary waves in shallow water" Journal of the Acoustical Society Express Letters, in press.

[5] Grigorev V., Katsnelson B. "Fluctuations of high frequency acoustic signals in shallow water due to motion of internal soliton" Acoustical Physics, in press